GEOPHYSICAL RESEARCH LETTERS, VOL. 26, NO. 24, PAGES 3601-3604, DECEMBER 15, 1999

Parallel electric fields in dispersive shear Alfvén waves in the dipolar magnetosphere

R. Rankin, J. C. Samson and V. T. Tikhonchuk[1]

Abstract. Existing theories do not explain large parallel electric fields that are associated with keV electron precipitation in auroral arcs. The MHD electron response results in an electrical conductivity in the low altitude magnetosphere that is two orders of magnitude greater than is required. We suggest a new mechanism for forming parallel electric fields based on a nonlocal electron response to standing shear Alfvén waves on dipole magnetic fields. Electron trapping is the primary cause of a significant reduction in the collisionless electron conductivity and consequent enhancement of parallel electric fields in the $1-4$ mHz frequency range.

Introduction

Discrete auroral arcs are produced by electron precipitation and play an important role in magnetosphere-ionosphere coupling. The energy range of precipitating electrons varies up to 10's of keV and is associated with a characteristic 10 km wide inverted-V potential structure. Electric current densities up to 10's of μA/m^2 have been inferred from ground based optical observations [*Samson et al.*, 1996] and measured directly in recent spacecraft missions such as FAST and FREJA [*Carlson et al.*, 1998; *Karlsson and Marklund*, 1996]. The acceleration region has been placed in the polar magnetosphere at altitudes ranging up to $1-2\,R_e$. There is no consensus on the precise nature of the accelerator, although different theories of discrete arcs have emerged. The key problem is to find a process that supports the required parallel electric current and parallel electric field of the order of mV/m. A relationship between a DC current and potential drop along geomagnetic field lines due to the magnetic mirror force has been obtained by *Knight* [1973] but the processes causing this potential drop have not been identified. Parallel electric fields have been considered by *Chiu and Schulz* [1978] also within an electrostatic approximation. However the parallel potential drop is on the order of the electron temperature in the plasma sheet, which is a free parameter in this model.

Discrete arcs are often associated with standing shear Alfvén waves (SAWs) in the mHz frequency range. External processes, such as solar wind pressure pulses, are assumed to drive SAWs to large amplitude on L-shells that intersect the equatorial magnetosphere at distances between $7-15R_e$. Dispersive effects in SAWs are necessary to generate the parallel electric field that is associated with electron acceleration. Theoretical models of dispersive SAWs have been advanced by *Rankin et al.* [1999] and *Streltsov and Lotko* [1999]. In a linear model, *Streltsov and Lotko* [1999] described a FAST observation of a field line resonance and obtained large electric fields by imposing an anomalous resistive layer at an altitude of 1 R_e above the ionospheres.

The nonlinear MHD model of dispersive SAWs by *Rankin et al.* [1999] is in good agreement with FAST observations of the primary acceleration region in terms of wave magnetic fields and parallel electric currents. This model also explains the formation of density cavities due to the SAW ponderomotive force. Cavities have been observed by satellites, [*Lundin et al.* 1994], and are considered an essential part of the acceleration process. However, because of very high wave conductivities, the parallel electric fields are a few orders of magnitude less than is required.

We show that a conventional two-fluid MHD description of collisionless parallel electron dynamics breaks down in a dipolar magnetic field and that kinetic effects lead to a nonlocal parallel conductivity that becomes very low at the expected location of the accelerator. The conductivity is strongly dependent on the distribution of trapped electrons and becomes particularly small in density cavities, where large electric fields are generated. These electric fields are not related to turbulent dissipation and can explain electron energization without making *a piori* assumptions.

Parallel Conductivity in Dispersive SAWs

First, we consider obstacles to the generation of large electric fields by SAWs. The energy of precipitating electrons is in the keV range and the acceleration length is roughly 1 R_e near the foot of geomagnetic field lines. This provides a figure of merit for parallel electric fields: $E_\parallel \sim 1$ mV/m. For field aligned currents $j_\parallel \sim 1$ μA/m^2, this requires a conductivity $\sigma = j_\parallel/E_\parallel \approx 10^{-3}$ S/m in a plasma with an average electron number density of 1 cm^{-3}.

Classical collisions give an electron conductivity, $\sigma = e^2 n_e/m_e\nu$, that is many orders of magnitude too large. One might appeal to an anomalous collision frequency [*Streltsov and Lotko*, 1999], which requires $\nu_{ef} \approx 30$ s^{-1}. In this case, the dissipation rate of electrons, $k_\perp^2/\mu_0\sigma_{ef}$, can easily exceed the SAW frequency and so it is interesting to consider first a collisionless kinetic conductivity model.

At low altitudes, parallel electric fields are attributed to electron inertia. This results in a reactive conductivity which depends on the SAW frequency, ω. The relation between the electron current and electric field follows from the electron momentum equation: $j_\parallel = ie^2 n_e E_\parallel/m_e\omega$. However, for observed SAW frequencies around 1.3 mHz, the inferred conductivity $|\sigma| = e^2 n_e/m_e\omega \approx 3$ S/m is too large.

For standing, dispersive SAWs in the equatorial magnetosphere, the electric field can be estimated from electron

[1]On leave from P. N. Lebedev Physics Institute, Russian Academy of Science, Moscow, Russia

Paper number 1999GL010715.
0094-8276/99/1999GL010715$05.00

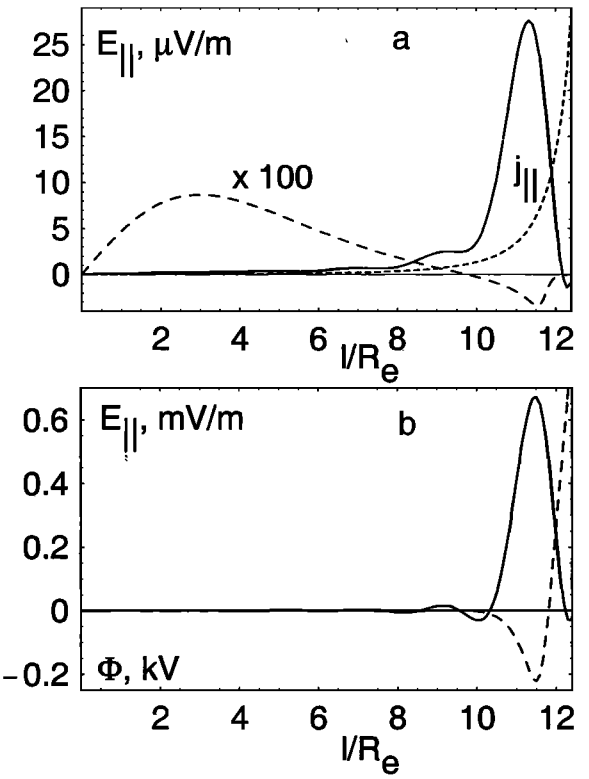

Figure 1. Distribution of the parallel SAW electric field (solid lines) along a dipolar magnetic field line $L = 10$; current amplitude 1 μA/m^2; $l = 0$ corresponds to the equatorial plane and the ionospheric end is at 12.6 R_e. Notice the different scales in panels (a) and (b). Panel (a) corresponds to the density profile (6) and panel (b) corresponds to the case with the density cavity. Dashed curve in panel (a) presents the wave electric field obtained in the MHD approximation, it is upscaled for comparison. Dotted line in panel (a) shows the profile of the field aligned current in arbitrary units shifted by one quarter of a wave period. Dashed line in panel (b) shows the profile of the static potential.

pressure balance: $E_\parallel \approx -\nabla_\parallel P_e/en_e$. On further assuming that electrons are isothermal, and using the electron continuity equation, one obtains in this case

$$\sigma \approx -i\frac{e^2 n_e}{m_e \omega}\left(\frac{\omega l_L}{V_{Te}}\right)^2 \qquad (1)$$

where l_L is the length of an L-shell field line and ωl_L for the SAW can be approximated by the Alfvén speed at the equatorial plane, $V_{A\,eq}$. Using our earlier estimates, and noting that $V_{A\,eq}/V_{Te} \sim 0.1$, we obtain an upper limit for $|\sigma| \approx 0.03$ S/m. This is an improvement over our previous estimates, but is still more than an order of magnitude too large. Furthermore, this conductivity is based on estimates near the equatorial magnetosphere, and is therefore in the wrong location for the accelerator. This is demonstrated in Fig. 1a, where the dashed curve shows $E_\parallel$ computed according to the MHD model described in *Rankin et al.* [1999].

The solution to the conductivity problem can be identified by considering the motion of electrons along geomagnetic field lines. This motion is influenced by the geomagnetic field, B, and by an electrostatic potential, Φ, that is required to support the electron density distribution along the field line. The latter can be described by a Boltzmann relation of the form $n_e(l) = n_{eq} \exp[e\Phi(l)/T_e]$; the electron temperature, T_e, is assumed to be constant, and n_{eq} is the equatorial number density of electrons. Neglecting the drift across magnetic shells, the electrons have two constants of motion, one being their total energy $w = m_e v^2/2 - e\Phi$, and the other being their magnetic moment $\mu = m_e v_\perp^2/2B$. The electron velocity along the field line can therefore be written as $v_\parallel = \sqrt{(2/m_e)(w - \mu B + e\Phi)}$, and for given w and μ will go to zero at different points along the field line. Since the geomagnetic field increases toward the ionosphere, most of the electrons are trapped near the equatorial region. However, a few electrons are still able to penetrate to the low altitude magnetosphere, where the field aligned current density increases due to the convergence of dipolar magnetic field lines. The current carriers deficiency near the foot of the field line must be supported by a correspondingly large parallel electric field.

Electron Parallel Conductivity

The electron conductivity involves nonlocal particle dynamics and requires a kinetic treatment. The electron gyrokinetic equation in the low frequency approximation has been derived in *Antonsen and Lane* [1980]. The SAW parallel electric field is regarded as a perturbation to the electron background state, f_{e0}, assumed to be Maxwellian, and the perturbation of the electron distribution function averaged over the electron gyration period evolves according to,

$$(-i\omega \pm v_\parallel \partial_l)\,\delta f_{e\pm} = \pm eE_\parallel v_\parallel \partial_w f_{e0} \qquad (2)$$

where $\pm$ is the sign of the electron velocity with respect to the guiding magnetic field and it has been assumed that $\delta f_{e\pm}$ oscillates with the SAW frequency. We consider here a quasistatic limit where the wave frequency is much smaller than the characteristic electron bounce frequency, V_{Te}/l_L. At the ionosphere, the electron distribution function and current are assumed to be continuous across the boundary.

Equation (2) is complicated due to the coordinate dependence of the electron velocity and must be solved on segments of a magnetic field line between electron turning points, l_t, corresponding to $v_\parallel = 0$, for trapped electrons, or between the turning point and the end of the magnetic field line for electrons on open orbits. The turning points depend on w and μ, and the current $j_\parallel = -ie\int d^3v v_\parallel \delta f_a$ depends on details of the antisymmetric part of the perturbed distribution function, $\delta f_a = (\delta f_{e+} - \delta f_{e-})/2i$, which is itself a function of $E_\parallel$. However, the SAW current is inductively produced and does not require details of the electron distribution function. Therefore, we are free to compute $j_\parallel$ using two-fluid MHD, but are forced to solve the inverse problem of finding $E_\parallel$ from Eq. (2). This is opposite to what is done in the DC model of *Knight* [1973].

To proceed, we expand both the current and electric field in a full set of basis functions along a magnetic field line. Non-periodic boundary conditions at the ionosphere suggest that we use Legendre polynomials, $P_n(l/l_L)$, with a weight function $B(l)$ that accounts for the geometric convergence of geomagnetic field lines. The current is therefore represented as

$$j_\parallel(l,t) = B(l)\sum j_n P_n \exp(-i\omega t) \qquad (3)$$

while a similar expansion, without the factor $B(l)$, is used for the electric field with coefficients e_n that are related to j_n through the conductivity matrix:

$$j_n = -i\frac{e^2 n_{eq}}{m_e \omega}\sum \hat{\sigma}_{nm} e_m \,. \qquad (4)$$

The dimensionless matrix $\hat{\sigma}$ is symmetric and can be expressed in the form:

$$\hat{\sigma}_{nm} = \frac{\omega l_L B_{eq}}{V_{Te} T_e^2}\int_{-e\Phi_{max}}^{\infty} dw\, e^{-w/T_e}\int_0^{\mu_{max}} d\mu\, Q_{nm} \,. \qquad (5)$$

Here, $\Phi_{max} = \Phi(l_L)$ is the maximum of the static electric potential, and $\mu_{max}(w) = \max\,[w + e\Phi(l)]/B(l)$ is the maximum magnetic moment that an electron with a given energy may attain. The dimensionless elements $Q_{nm}(w,\mu)$ are defined by

$$\begin{aligned} Q_{nm} \;=\; & \frac{\sqrt{2/\pi}}{\Theta[\omega\tau(l_{t1},l_{t2})]}\int_{l_{t1}}^{l_{t2}}\frac{dl}{l_L}P_n(l)\times \\ & \left\{\Theta[\omega\tau(l,l_{t2})]\int_{l_{t1}}^{l}\frac{dl'}{l_L}P_m(l')\,\sin\omega\tau(l_{t1},l')+\right. \\ & \left.\sin\omega\tau(l_{t1},l)\int_{l}^{l_{t2}}\frac{dl'}{l_L}P_m(l')\,\Theta[\omega\tau(l',l_{t2})]\right\} \end{aligned}$$

where Θ is a cosine function for electrons on open orbits and is a sine function for trapped electrons. The electron travel time between the points l_1 and l_2 along an electron orbit is defined by the function $\tau(l_1,l_2) = \int_{l_1}^{l_2} dl/v_\parallel$. Turning points satisfying $-l_L < l_{t1} < l_{t2} < l_L$ correspond to trapped electrons, while $l_{t1} = -l_L$ or $l_{t2} = l_L$ corresponds to electrons on open orbits. The integrals contain poles corresponding to wave damping associated with resonance particles with a bounce time comparable to the wave period. This damping is weak for the low wave frequencies considered here, and is neglected in the numerical calculations presented below.

The evaluation of the conductivity matrix in Eq. (5) is the main technical task remaining. Once the coefficients are known, the electric field can be found provided the current profile is specified. We will not elaborate the details of the conductivity calculations, but will rather describe specific examples and discuss the main findings of our analysis.

Analysis and Discussion

Two major factors affect the SAW conductivity in a dipolar magnetic field. The first is a geometric effect: The SAW current is highly peaked near the ionosphere because of the convergence of geomagnetic field lines. The electric field is also concentrated near the ionospheres and this corresponds to an effective reduction of the conductivity. The second effect is due to the magnetic mirror force: The dominant contribution to the conductivity comes from electron orbits with $v_\parallel \lesssim \omega l_L$, where the electron bounce time is large, and from open orbits. There are no such orbits if the magnetic moment is large and this is the reason for the conductivity inhibition in the case $\omega \ll V_{Te}/l_L$.

We consider a dipolar geomagnetic field line $L = 10$ and choose two density profiles: First, is a density profile which increases exponentially near the ionosphere:

$$n_e = n_{eq}\left(1 + 10^5 \exp\frac{r_{min} - r}{0.08 R_e}\right) \qquad (6)$$

where r is the geocentric distance and $r_{min} = 1.15 R_e$ is the position of the ionospheric end of the magnetic field line. A similar profile was used by [*Thompson and Lysak*, 1996] in their studies of electron acceleration by inertial Alfvén waves. The second profile is the same as (6) but with a 90% density depression at an altitude of $1.2R_e$ (cf. Fig. 1b). With $n_{eq} = 1$ cm^{-3} and an effective ion mass $m_i = 7$ amu the frequency of the fundamental SAW mode $\omega \approx 2.1 V_{A\,eq}/LR_e$ (1.3 mHz), and the ratio $\omega L R_e/V_{Te} \approx 0.13$ for an electron temperature $T_e = 100$ eV. (A somewhat unrealistic ion mass was chosen to lower the SAW frequency to the observed value within the dipolar magnetic field approximation.) The current profile corresponding to this fundamental mode can be seen in Fig. 1a (dotted line). It is essentially divergenceless for distances $l \gtrsim 4\,R_e$ and is practically the same for both density profiles.

The conductivity matrix has been calculated using up to 15 Legendre polynomials and the parallel electric field reconstructed from the inversion of Eq. (4). The results are shown as solid lines in Fig. 1 and the result achieved within the two-fluid MHD approximation is shown with a dashed line for comparison. In the kinetic calculation with the exponential density profile (6), the most significant differences from MHD are the large, approximately a factor of 300, enhancement of the electric field and shift of the maximum to the low altitude part of the field line. The effective conductivity can be estimated as the ratio of the maxima of the electric current and the parallel electric field. This provides the estimate of 0.03 S/m. For a peak current density of $1\,\mu$A/m^2, the parallel potential drop $\Phi_\parallel$ is about 260 V. The maximum of the electric field is at an altitude of $1.4R_e$; its full width at half maximum is $1.2R_e$, and its subsequent decrease toward the ionosphere is due to the exponential increase of plasma density.

The case with a plasma density cavity is shown in Fig. 1b. The dashed line shows the static potential, $\Phi = (T_e/e)\ln(n_e/n_{eq})$. There is more than an order of magnitude increase in the wave electric field amplitude as compared to the exponential profile. The maximum electric field of 0.7 mV/m is achieved at the bottom of the density cavity. This corresponds to an effective electric conductivity of 10^{-3} S/m.

An estimate for the parallel wave potential can be obtained for the special case of constant density, if one accounts for the fact that most of the electric potential drop is localized to a small portion of the field line and that only the precipitating electrons on open orbits carry the current at the foot of the magnetic field line:

$$j_{max} \approx i\,(e^2 n_{eq}\omega l_L/T_e)\,\Phi_\parallel \,. \qquad (7)$$

Here, $-\Phi_\parallel = \int E_\parallel dl \sim E_{max}\Delta l$. Compared to Eq. (1) this expression results in a conductivity that is smaller by a factor $l_L/\Delta l$ because of the peaked distribution of the electric field. The plasma conductance that follows from Eq. (7) is $V_{Te}/\omega l_L$ times less than that suggested by *Knight* [1973] in his model of DC current. For typical magnetospheric parameters it is about 1 nS/m^2. The potential drop in the case shown in Fig. 1b is about 4.3 kV, which agrees with Eq. (7).

Conclusions

The MHD approximation leads to a substantial underestimate of SAW dispersive parallel electric fields on low altitude high latitude geomagnetic field lines. The nonlocal electron response to parallel currents produced by SAWs

can account for a significant decrease of the electron conductivity, especially in cases where the background density is severely depleted. The SAW conductivity has been calculated using the electron gyrokinetic equation and the field aligned electron current computed from the eigenfunction for SAWs in a dipole field. This is a self-consistent model which takes into account dispersive effects in SAWs, the presence of trapped electrons, and wave damping. Unlike static models [*Knight,*, 1973; *Chiu and Schulz,* 1978] it accounts self-consistently for both trapped and loss cone electrons and does not require anisotropic hot electron and ion populations in the equatorial plane. Since the ion response has been neglected in our model, it is restricted to the frequency range $V_{Ti}/l_L < \omega < V_{Te}/l_L$ which corresponds to the ULF frequency range in Earth's magnetosphere. Our perturbation theory also requires that we neglect the effect of cold return electrons from the ionosphere. These limitations remain to be investigated.

With a field aligned current magnitude of 1 μA/m^2, and plasma conditions appropriate to $L = 10$ auroral field lines, the low altitude SAW parallel electric field is enhanced by more than two orders of magnitude compared to the MHD electron response. A low altitude density minimum along the geomagnetic field leads to a further significant increase in the parallel electric field, bringing it to the mV/m range. Such density cavities have been observed and shown to be consistent with excitation by the ponderomotive force of SAWs. Therefore, shear Alfvén waves provide a self-consistent model of time-modulated discrete auroral arc formation and energetic particle precipitation in the auroral zone.

Acknowledgments. Research supported by the Canadian Space Agency, NSERC, and Russian Foundation for Basic Research, grant No. 99-02-17267. Authors also acknowledge Gorman Ho who implemented many of the numerical computations.

References

Antonsen, T. M., and B. Lane, Kinetic calculations for low frequency instabilities in inhomogeneous plasmas, *Phys. Fluids, 23,* 1205, 1980.

Carlson, C. W., R. F. Pfaff, and J. G. Watson, The Fast Auroral SnapshoT (FAST) mission, *Geophys. Res. Lett., 25,* 2013, 1998.

Chiu, Y. T., and M. Schulz, Self-consistent particle and parallel electrostatic field distributions in the magnetospheric-ionospheric auroral region, *J. Geophys. Res., 83,* 629, 1978.

Karlsson, T., and G. T. Marklund, A statistical study of intense low- altitude electric fields observed by Freja, *Geophys. Res. Lett., 23,* 1005, 1996.

Knight, S., Parallel electric fields, *Planet. Space Sci., 21,* 741, 1973.

Lundin, R., L. Eliasson, G. Haerendel, M. Boehm, and B. Holback, Large scale auroral density cavities observed by Freja, *Geophys. Res. Lett., 21,* 1903, 1994.

Rankin, R., J. C. Samson, and V. T. Tikhonchuk, Discrete auroral arcs and nonlinear dispersive field line resonances, *Geophys. Res. Lett., 26,* 663, 1999.

Samson, J. C., L. L. Cogger, and Q. Pao, Observations of field line resonances, auroral arcs and auroral vortex structures, *J. Geophys. Res., 101,* 17373, 1996.

Streltsov, A., and W. Lotko, Small scale, "electrostatic" auroral structures and Alfvén waves, *J. Geophys. Res., 104,* 4411, 1999.

Thompson, B. J., and R. L. Lysak, Electron acceleration by inertial Alfvén waves, *J. Geophys. Res., 101,* 5359, 1996.

R. Rankin, J. C. Samson, V. T. Tikhonchuk, Department of Physics, University of Alberta, Edmonton, Alberta, Canada T6G 2E9. (e-mail: rankin@space.ualberta.ca; samson@space.ualberta.ca; tikhon@space.ualberta.ca)

(Received July 24, 1999; revised September 14, 1999; accepted September 23, 1999.)